

# Computational Modelling and Simulation of the Human Duodenum

Bostjan Hari<sup>\*1</sup>, Serafim Bakalis<sup>1</sup>, and Peter Fryer<sup>1</sup>

<sup>1</sup>The University of Birmingham, School of Chemical Engineering

\*Corresponding author: Edgbaston, Birmingham B15 2TT, United Kingdom, b.hari@bham.ac.uk

**Abstract:** Worldwide attention in the computational modelling and simulation of the human intestine is increasing in order to help understand its complex behaviour and improve health [1,2,3]. Computational fluid dynamics (CFD) is an essential tool to understand the mechanics and transport phenomena of the intestine, thereby advancing the diagnosis and treatment of gastrointestinal related diseases. The aim of this work is to develop a computational model of the human duodenum. The CFD model couples peristaltic motions of the duodenum wall together with the flow of chyme, known as a fluid – structure interaction coupling. The fluid flow of chyme is described by Navier – Stokes equations, while the duodenum contractions are approximated by the smoothed Heaviside step function. Mixing of chyme, caused by peristalsis, is modelled with the particle tracing module. A hydrolysis of starch, producing glucose, is added to the convection – diffusion equation to observe the flux of glucose through the duodenum wall.

**Keywords:** Human duodenum, peristaltic movements, fluid - structure interaction, computational fluid dynamics, COMSOL Multiphysics.

## 1. Introduction

The human duodenum is part of the small intestine to the stomach through the pylorus. It takes the form of a C shaped tube, which is connected to the pancreas and mixes chyme from the stomach with digestive juices secreted from the pancreas and liver. The pancreatic juice also contains sodium bicarbonate, which neutralises stomach acid in the chyme. The pancreas produces and secretes a variety of digestive enzymes into the duodenum, which break down starches, lipids and proteins. The muscular layers of the digestive tract consist of smooth muscle tissue, which trigger peristaltic and segmentation movements. Peristalsis propels a small mass of digestive contents called a bolus along the length of digestive tract. The small intestine undergoes

cycles of contractions that chop the bolus and mix the intestine contents with pancreatic juices. This activity is called segmentation and does not follow the same pattern as peristalsis [4].

The chyme along the duodenum-like porous tube is transported by peristaltic waves. Our simplified duodenum model consists of starch only, which reacts with water and breaks down into glucose. Produced glucose is further absorbed through the duodenum-like porous wall into the simulated bloodstream.

Figure 1 shows geometry and boundary conditions of the duodenum-like porous and elastic silicone tube. It consists of domain 1 and domain 2. Domain 1 is a fluid flow channel made of porous and elastic silicone tube, whereas domain 2 represents a porous wall of the elastic silicone tube.

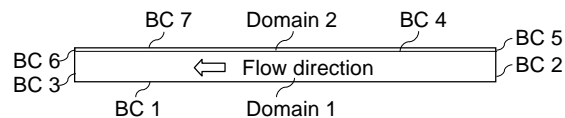


**Figure 1.** Boundary conditions of the duodenum-like elastic silicone tube.

The duodenum-like porous tube is modelled with the finite element method, used in COMSOL Multiphysics, as an axis symmetric computational mesh made of quadrilateral elements.

## 2. Use of COMSOL Multiphysics

The CFD model of the human duodenum is modelled with COMSOL Multiphysics 4.2a. It consists of five different interfaces and related equations found in [5], which are briefly explained below.

The first interface, Free and Porous Media Flow, describes the laminar Newtonian fluid flow of chyme in the main flow channel, whereas the Brinkman equations model the fluid flow through the porous duodenum wall.

The laminar flow of chyme in domain 1 is described by Navier – Stokes equations and continuity equation

$$\rho \partial \mathbf{u}_f / \partial t + \rho (\mathbf{u}_f \cdot \nabla) \mathbf{u}_f = \nabla \cdot [-p \mathbf{I} + \mu (\nabla \mathbf{u}_f + (\nabla \mathbf{u}_f)^T)]$$

$$\rho \nabla \cdot \mathbf{u}_f = 0$$

where  $\rho$  [kg/m<sup>3</sup>] is the density of the fluid,  $\mathbf{u}_f$  [m/s] is the velocity vector of the fluid,  $p$  [Pa] is the pressure of the fluid,  $\mathbf{I}$  [-] is the identity matrix,  $\mu$  [Pa·s] is the dynamic viscosity of the fluid and  $t$  [s] is time.

The fluid or chyme, together with glucose, can penetrate through the duodenum wall into the bloodstream. Thus, the Brinkman equations and the continuity equation are applied to the porous duodenum wall, represented by domain 2, as

$$\rho / \varepsilon_p [\partial \mathbf{u}_f / \partial t + (\mathbf{u}_f \cdot \nabla) \mathbf{u}_f / \varepsilon_p] = \nabla \cdot [-p \mathbf{I} + \mu / \varepsilon_p (\nabla \mathbf{u}_f + (\nabla \mathbf{u}_f)^T)] - 2\mu / 3\varepsilon_p (\nabla \cdot \mathbf{u}_f) \mathbf{I} - (\mu / \kappa_{br} + \beta_F |\mathbf{u}_f| + Q_{br}) \mathbf{u}_f$$

$$\rho \nabla \cdot \mathbf{u}_f = 0$$

where  $\varepsilon_p$  [-] is the porosity of the duodenum wall modelled with silicone tube,  $\kappa_{br}$  [m<sup>2</sup>] is the permeability of the silicone tube,  $\mu$  [Pa·s] is the dynamic viscosity of the fluid,  $\beta_F$  [kg/m<sup>4</sup>] is the Forchheimer term and  $Q_{br}$  [kg/m<sup>3</sup>·s] is a mass source or mass sink.

The second interface, Solid Mechanics, applies the smoothed Heaviside step function and external load to mimic peristaltic movements of the silicone tube.

The governing equations of linear elasticity needed to model duodenum-like elastic and porous silicone tube are presented by the linear elastic material model and are based on Newton's second law of motion

$$\rho_m (\partial^2 \mathbf{u}_{dis} / \partial t^2) - \nabla \cdot \boldsymbol{\sigma} = \mathbf{F}_v$$

where  $\rho_m$  [kg/m<sup>3</sup>] is the density of the elastic silicone tube,  $\mathbf{u}_{dis}$  [m] is the displacement vector,  $\boldsymbol{\sigma}$  [N/m<sup>2</sup>] is the normal Cauchy stress tensor that relates stresses in the silicone tube and  $\mathbf{F}_v$  [N/m<sup>3</sup>] is the body force per unit volume.

The Cauchy stress tensor can be written

$$\boldsymbol{\sigma} = j^{-1} \mathbf{F} \mathbf{S} \mathbf{F}^T$$

where  $\mathbf{F}$  [m] is the deformation gradient tensor,  $\mathbf{F}^T$  [m] is the transposed deformation gradient tensor,  $\mathbf{S}$  [N/m<sup>2</sup>] is the second Piola – Kirchhoff stress tensor that relates forces to areas in the duodenum-like silicone tube and  $j$  [-] is the determinant of tensor  $\mathbf{F}$  called Jacobian matrix. The deformation gradient tensor is defined as

$$\mathbf{F} = \mathbf{I} + \nabla \mathbf{u}_{dis}$$

where  $\mathbf{I}$  [-] is the identity matrix and  $\nabla \mathbf{u}_{dis}$  [m] is the material displacement gradient vector.

When the external load is applied to the silicone tube, the force causes deformation to the material. The displacement gradient is thus

$$\boldsymbol{\varepsilon} = 1/2 [(\nabla \mathbf{u}_{dis})^T + \nabla \mathbf{u}_{dis} + (\nabla \mathbf{u}_{dis})^T \nabla \mathbf{u}_{dis}]$$

where  $\boldsymbol{\varepsilon}$  [-] is the infinitesimal strain tensor.

Behaviour of elastic materials is represented by Duhamel – Hooke's law and relates the normal stress tensor to the strain tensor. Elasticity tensor  $\mathbf{C}$  [N/m<sup>2</sup>] is represented by Duhamel – Hooke equation and is function of Young's modulus  $E$  [N/m<sup>2</sup>] and Poisson's ratio  $\nu$  [-].

The load  $\mathbf{F}_{A,r}$  [N/m<sup>2</sup>] in the radial direction applied to the elastic silicone tube is

$$\mathbf{F}_{A,r} = -L_{max} \cdot \text{load}(z_s, t_s)$$

where  $L_{max}$  [N/mm<sup>2</sup>] is the maximum load applied to the silicone tube, load is the Heaviside function and  $z_s$  [-] and  $t_s$  [-] are the dimensionless function arguments.

The third interface, Moving Mesh, adds mesh displacements and velocities to the existing model and couples the second and the first interfaces into the complex fluid – structure interaction computational model.

Mesh deformation is caused by the load applied to the elastic tube and by peristaltic waves modelled by Heaviside function.

The fourth interface, Particle Tracing for Fluid Flow, contributes to the duodenum model by tracing solid particles and their mixing with the fluid flow.

The motion of particles in a fluid flow is described with Newton's Second Law

$$d(m_p \mathbf{u}_p)/dt = \mathbf{F}_D$$

where  $m_p$  [kg] is the particle mass,  $\mathbf{F}_D$  [N] is the vector of the force exerted on the particle and  $\mathbf{u}_p$  [m/s] is the velocity vector of the particle. The drag force is the only force acting on individual particle, if no other forces are applied

$$\mathbf{F}_D = m_p F_d (\mathbf{u}_f - \mathbf{u}_p)$$

where  $F_d$  [N] is the drag force per unit mass and  $\mathbf{u}_f$  [m/s] is the velocity vector of the fluid. The drag force per unit mass for spherical particles in a laminar flow is defined as

$$F_d = 18\mu / (\rho_p d^2)$$

where  $\mu$  [Pa·s] is the dynamic viscosity of the fluid,  $\rho_p$  [kg/m<sup>3</sup>] is the particle density and  $d$  [m] is the particle diameter.

The fifth interface, Transport of Diluted Species, models convection and diffusion phenomena inside the silicone tube and in the porous wall together with the simplified hydrolysis reaction of starch producing glucose. Flow of chyme includes digested starch from mouth and stomach and reacts inside the human duodenum with gastric juices and digested enzymes. The unconverted starch reacts with digestive enzymes inside the duodenum where it is converted into glucose. The simplified reaction is written as



where  $c_s$  [mol/m<sup>3</sup>] and  $c_g$  [mol/m<sup>3</sup>] are the concentration of starch and glucose. The rate of reaction of starch and glucose are described as

$$-R_s = k \cdot c_s$$

$$R_g = k \cdot c_g$$

where  $R_s$  [mol/m<sup>3</sup>·s] and  $R_g$  [mol/m<sup>3</sup>·s] are the rate of reaction of starch and glucose and  $k$  [1/s] is the first order rate constant.

The phenomena of convection, diffusion and chemical reactions inside the human duodenum are described with convection – diffusion equations for starch and glucose

$$\partial c_s / \partial t + \nabla \cdot (-D_s \cdot \nabla c_s) + \mathbf{u}_f \cdot \nabla c_s = R_s$$

$$\partial c_g / \partial t + \nabla \cdot (-D_g \cdot \nabla c_g) + \mathbf{u}_f \cdot \nabla c_g = R_g$$

where  $D_s$  [m<sup>2</sup>/s] and  $D_g$  [m<sup>2</sup>/s] are diffusion coefficients of starch and glucose and  $\mathbf{u}_f$  [m/s] is the velocity vector of the fluid flow.

When diffusion and velocity are the transport mechanisms, the flux of glucose, through boundary 7 is described as

$$-\mathbf{n} \cdot (-D_g \cdot \nabla c_g + \mathbf{u}_f \cdot \nabla c_g) = k_g (c_{g,out} - c_{g,in})$$

where  $k_g$  [m/s] is the mass transfer coefficient and  $c_{g,out}$  [mol/m<sup>3</sup>] and  $c_{g,in}$  [mol/m<sup>3</sup>] are the bulk concentration of glucose in the bloodstream and on boundary 7 as computed by the CFD solver.

**Table 1.** Initial and boundary conditions applied to five interfaces modelled by COMSOL Multiphysics.

Physical Domains	Initial Conditions	SI Units
D 1,2	$u_z = 0$	[m/s]
D 1,2	$u_r = 0$	[m/s]
D 1,2	$p = 0$	[Pa]
D 2	$u_{2,z} = 0$	[m]
D 2	$u_{2,r} = 0$	[m]
D 2	$\partial u_{2,z} / \partial t = 0$	[m/s]
D 2	$\partial u_{2,r} / \partial t = 0$	[m/s]
D 1,2	$d_{0,z} = 0$	[m]
D 1,2	$d_{0,r} = 0$	[m]
D 1	$c_{0,s} = 31.176$	[mol/m <sup>3</sup> ]
D 1,2	$c_{0,g} = 0$	[mol/m <sup>3</sup> ]

Physical Boundaries	Boundary Conditions	SI Units
BC 2,3,5,6	$p_0 = 0$	[Pa]
BC 4	$u_w = 0$	[m/s]
BC 7	$u_{w,z} = \text{solid.u}_tZ$	[m/s]
BC 7	$u_{w,r} = \text{solid.u}_tR$	[m/s]
BC 4	$p = p$	[Pa]
BC 5,6	$w_{0,2} = 0$	[m]
BC 7	$F_{A,z} = 0$	[N/m <sup>2</sup> ]
BC 7	$F_{A,r} = F_{A,r}$	[N/m <sup>2</sup> ]
BC 1	$d_r = 0$	[m]
BC 2,3,5,6	$d_z = 0$	[m]
BC 4,7	$v_z = \text{solid.u}_tZ$	[m/s]
BC 4,7	$v_r = \text{solid.u}_tR$	[m/s]

BC 1,2,3,4	$x' = x_c$	[m]
BC 1,2,3,4	$v' = v_c$	[m/s]
BC 2,3,4	$-\mathbf{n} \cdot D_s \nabla c_s = 0$	[mol/m <sup>2</sup> s]
BC 2,3	$-\mathbf{n} \cdot D_g \nabla c_g = 0$	[mol/m <sup>2</sup> s]
BC 5,6	$-\mathbf{n} \cdot (D_g \nabla c_g + \mathbf{u}_f c_g) = 0$	[mol/m <sup>2</sup> s]
BC 7	$-\mathbf{n} \cdot (D_g \nabla c_g + \mathbf{u}_f c_g) = N_g$	[mol/m <sup>2</sup> s]

Each set of governing equations is computed separately in order to simplify the computational procedure. The Navier – Stokes equations and Brinkman equations from the Free and Porous Media Flow interface are solved together with the Solid Mechanics interface and Moving Mesh interface governing equations. The equations, which solve particle trajectories in the Particle Tracing for the Fluid Flow interface, are solved next. Velocity fields, needed in these set of equations, are used from the stored solution computed by the Free and Porous Media Flow interface. The Transport of Diluted Species interface uses the same stored velocity fields to solve convection – diffusion equations and compute concentration fields of starch and glucose in every cell of the computational mesh. A time dependent segregated solver solves the first set of governing equations defined in the Free and Porous Media Flow, Solid Mechanics and Moving Mesh interfaces. The set of equations, which describe particle movements in the Particle Tracing for Fluid Flow interface are solved with fully coupled time dependent solver, whereas the convection – diffusion equations within the Transport of Diluted Species interface are solved by direct time dependent solver.

### 3. Results

Figure 2 shows velocity snapshots of the fluid flow inside the duodenum-like elastic silicone tube, for dynamic viscosity 0.1 Pa·s and fluid density 970 kg/m<sup>3</sup>. The elastic silicone tube with Poisson ratio 0.48 and Young's modulus 1.0·10<sup>7</sup> Pa approximates the human duodenum. Peristaltic waves are modelled by applying a physical force to the silicone tube, which is applied 45 mm from the lower edge of the tube at time 0.8 s after the beginning of the simulation. The full strength is reached after 0.6 s and the load is disengaged after 3.4 s from the beginning of the simulation. The applied force

needs to be strong enough to squeeze the tube and push the fluid flow of chyme forward at the same time. According to several numerical attempts, the most appropriate force is 1.5·10<sup>5</sup> N/mm<sup>2</sup>. The direction of the fluid flow and peristaltic movements are from the bottom towards the top of the tube.

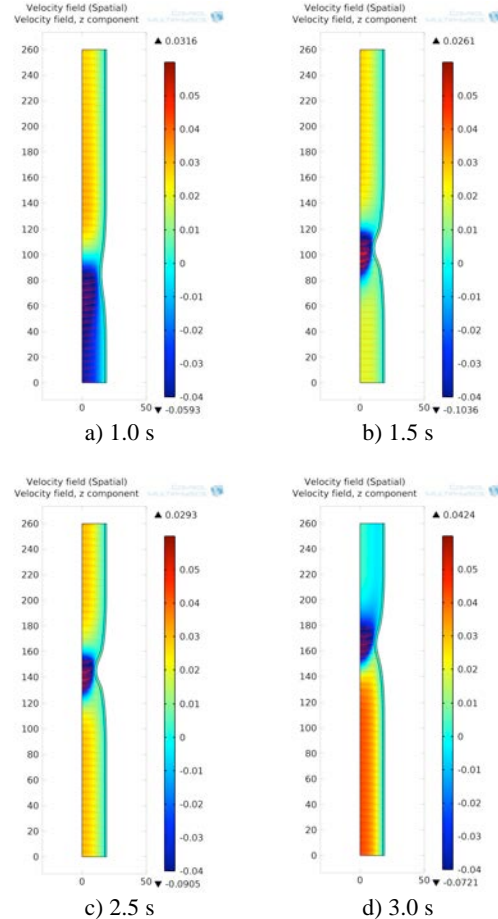


**Figure 2.** Velocity field in the axial direction [m/s] represented as surface plots and spatial direction of velocity fields represented as vector plots. The snapshots are taken for the Newtonian fluid flow at dynamic viscosity 0.1 Pa·s, density 970 kg/m<sup>3</sup>, Poisson ratio 0.48, Young's modulus 1.0·10<sup>7</sup> Pa and load 1.5·10<sup>5</sup> N/mm<sup>2</sup> at time steps 1.0 s, 1.5 s, 2.5 s and 3.0 s. The scale represents the minimum and maximum range of velocity field in the axial direction.

Figure 3 gives an overview of mixing inside the silicone tube, by tracing particle trajectories from their initial to final state in the space. All snapshots show 74 particles released from the

left hand side of the grid along the axis of symmetry at time zero. By increasing time step for 0.1 s, particles move towards the right hand side of the tube leaving a trail to form a trajectory. Each point on a newly formed trajectory represents a new position of an individual particle at certain time step. Intensity of mixing, presented with red colour, is the highest below the peristaltic wave.

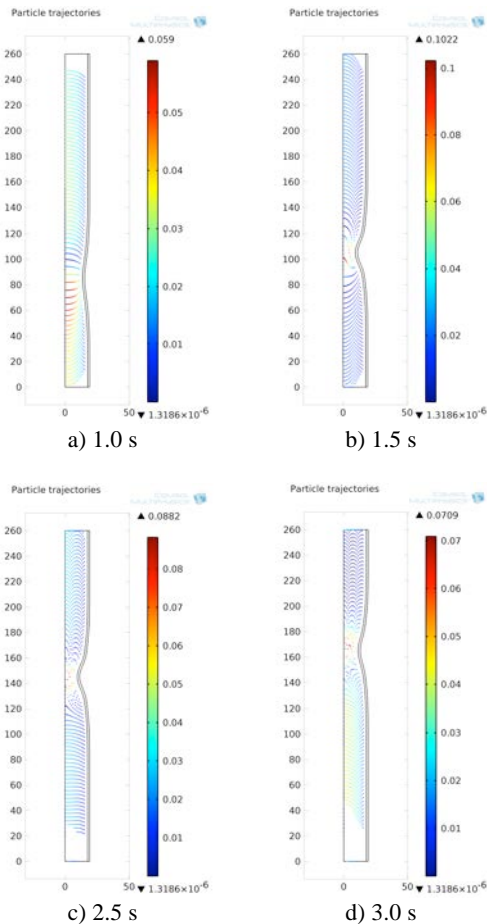


**Figure 3.** Particle trajectories of the fluid flow represented as surface plots. The snapshots are taken for the Newtonian fluid flow at dynamic viscosity 0.1 Pa·s, density 970 kg/m<sup>3</sup>, Poisson ratio 0.48, Young's modulus 1.0·10<sup>7</sup> Pa and load 1.5·10<sup>5</sup> N/mm<sup>2</sup> at time steps 1.0 s, 1.5 s, 2.5 s and 3.0 s. The scale represents the minimum and maximum range of particle velocities.

Figure 4 shows the concentration field of glucose inside the duodenum-like silicone tube and inward diffusive flux of glucose through the

duodenum-like porous wall. The reaction in this case study is a simplified hydrolysis reaction of starch producing glucose. As seen from figure 4b, glucose is initially produced from starch in the region of intense mixing after the peristaltic wave. The production of glucose advances around the wave by increasing the time step and spreads out to the neighbouring region. The diffusive flux of glucose through the duodenum wall is the highest around 3.0 s.

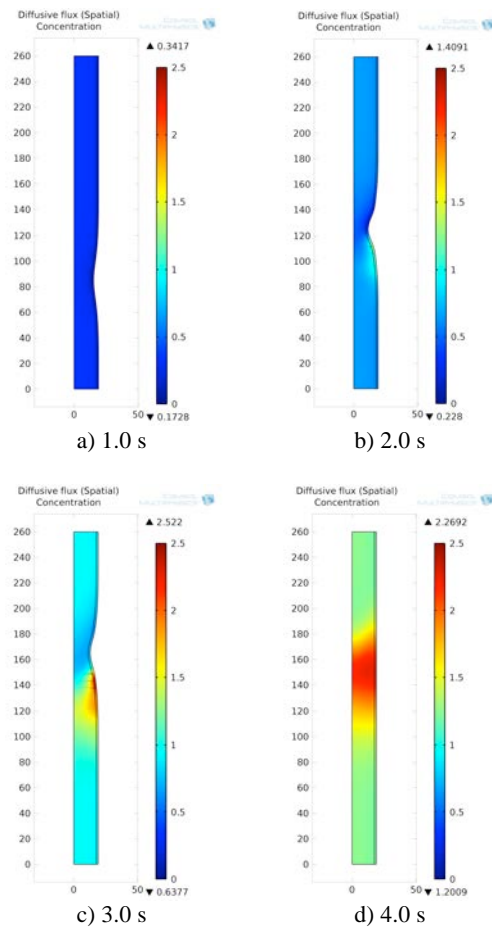


**Figure 4.** Concentration field of glucose [mol/m<sup>3</sup>] represented as surface plots and spatial inward diffusive flux of glucose through the porous silicone wall represented as vector plots. The snapshots are taken for the Newtonian fluid flow at dynamic viscosity 0.1 Pa·s, density 970 kg/m<sup>3</sup>, Poisson ratio 0.48, Young's modulus 1.0·10<sup>7</sup> Pa and load 1.5·10<sup>5</sup> N/mm<sup>2</sup> at time steps 1.0 s, 2.0 s, 3.0 s and 4.0 s. The scale represents the minimum and maximum range of the glucose concentration field.

#### 4. Conclusions

A computational fluid - structure interaction duodenum model that mimics peristaltic movements, chyme fluid flow, mixing and absorption of glucose through the porous duodenum wall has been developed. The future work will validate computational results obtained by the in-silico duodenum model against the experimental results obtained by the in-vitro duodenum prototype.

#### 5. References

1. M. Taghipoor, P. Lescoat, J.-R. Licois, C. Georgelin, G. Barles, Mathematical Modeling of Transport and Degradation of Feedstuffs in the Small Intestine, *Journal of Theoretical Biology*, **294**, 114-121 (2012).
2. A. Tharakan, I. T. Norton, P. J. Fryer, S. Bakalis, Mass Transfer and Nutrient Absorption in a Simulated Model of Small Intestine, *Journal of Food Science*, **75**, E339-E346 (2010).
3. B. R. Stoll, R. P. Batycky, H. R. Leipold, S. Milstein, D. A. Edwards, A Theory of Molecular Absorption from the Small Intestine, *Chemical Engineering Science*, **55**, 473-489 (2000).
4. G. J. Tortora, B. H. Derrickson, *Principles of Anatomy and Physiology, Volume 2 – Maintenance and Continuity of the Human Body, 12<sup>th</sup> International Student Edition*, 1174, John Wiley & Sons, Inc. (2009).
5. COMSOL Multiphysics 4.2a Help – Online Documentation, COMSOL AB (2012).

#### 6. Acknowledgements

The authors gratefully acknowledge support of the Biotechnology and Biological Sciences Research Council (BBSRC) from the United Kingdom for funding the project with the reference BB/I006079/1 and COMSOL AB from Sweden for technical support with COMSOL Multiphysics 4.2a software.